Int. J. Heat Mass Transfer. Vol. 34, No. 2, pp. 357–367, 1991
Printed in Great Britain

0017-9310/91 \$3.00+0.00

A unified similarity transformation for free, forced and mixed convection in Darcy and non-Darcy porous media

A. NAKAYAMA
Department of Energy and Mechanical Engineering, Shizuoka University, 3-5-1 Johoku, Hamamatsu 432, Japan

and

I. POP
Faculty of Mathematics, University of Cluj, R-3400 Cluj, CP 235, Romania

(*Received* 10 *November* 1989 *and in final form* 1 *February* 1990)

Abstract—A unified similarity transformation is proposed to extract all possible similarity solutions for free, forced and mixed convection within Darcy and non-Darcy porous media. The slip velocity at the wall resulting from both the externally forced flow and the buoyancy force is chosen as a velocity scale to form a modified Peclet number which naturally transforms into the conventional Peclet number and Rayleigh number under certain physical limiting conditions. This unified treatment reveals three limiting flow regimes, namely, the forced convection regime, the Darcy free convection regime and the Forchheimer free convection regime, as well as three other intermediate flow regimes, namely, the Darcy mixed convection regime, the Darcy–Forchheimer free convection regime and the Forchheimer mixed convection regime. Relevant flow parameters for distinguishing these flow regimes are found to be the 'micro-scale' Reynolds and Grashof numbers based on the square root of the permeability. A flow regime map has been constructed to show these six different flow regimes, taking the two micro-scale dimensionless numbers as the abscissa and ordinate variables, Asymptotic expressions derived for these flow regimes appear quite useful for practical estimation of convective heat transfer within Darcy and non-Darcy porous media.

INTRODUCTION

MOST of the studies devoted to the field of convective flow within porous media are based on the Darcy flow model, in which the pressure gradient is assumed to be in proportion to an apparent velocity, namely, the Darcian velocity. The initial work on Darcian free convection over a vertical flat surface was carried out by Cheng and Minkowycz [1], while Nakayama and Koyama [2] generalized the similarity transformation proposed by Merkin [3], for Darcian free convection over a non-isothermal body of arbitrary shape. Mixed convection problems were also attacked by some workers, using the Darcy flow model. Similarity solutions have been found for the mixed convection flow over isothermal bodies [4] and non-isothermal bodies [5] placed in a fluid-saturated porous medium.

It is, however, well known that the Darcy flow model breaks down, when the inertia resistance (owing to wake and separation bubbles formed behind a micro-structure) becomes comparable to the viscous (Darcy) resistance. Forchheimer [6] proposed a quadratic term in Darcian velocity to describe the inertia effects. Bejan and Poulikakos [7] pointed out that this non-Darcy flow model should be employed for all high velocity flows in porous media with low permeability, if we are to resolve the conflict, namely, that the Darcy flow model deteriorates as the boundary layer approximation improves, and vice versa. Plumb and Huenefeld [8] attacked non-Darcian free convection over a vertical isothermal flat plate. Their work was followed by Nakayama *et al.* [9] to study possible geometries and their corresponding wall temperature distributions, which permit similarity solutions. Non-Darcy free convection from a vertical plate with mass transfer was treated by Kumari *et al.* [10], while non-Darcy free convection over a slender vertical frustum of a cone was investigated by Vasantha *et al.* [11]. The studies of non-Darcy mixed convection, on the other hand, have been limited only for a horizontal flat surface [12] and a vertical cylinder [13], so far.

In this paper, we shall present a unified similarity transformation procedure which yields classes of possible similarity solutions for free, forced and mixed convection of Darcian and non-Darcian fluids. Almost all similarity solutions already reported in the literature are readily reducible from the present set of general differential equations. Another new class of similarity solutions is also found in the Forchheimer flow regime where the flow is so strong that the Darcy resistance is negligible when compared with the inertia resistance. This unified similarity treatment reveals that there exist three limiting flow regimes, namely,

NOMENCLATURE

C	empirical constant associated with porous inertia
f	dimensionless stream function
g_x	tangential component of acceleration due to gravity
Gr^*	micro-scale Grashof number, defined in equation (10b)
I	function defined in equation (19)
k	thermal conductivity
K	permeability
m	exponent associated with the free stream velocity, $u_e \propto x^m$
n	exponent associated with the wall temperature, defined in equation (25)
Nu_x	local Nusselt number, defined in equation (27)
p	pressure
Pe_x	local Peclet number, defined in equation (12a)
Pe_x^*	modified Peclet number, defined in equation (13)
q_w	wall heat flux
r	function representing wall geometry
r^*	1 for plane flow and r for axisymmetric flow
Ra_x	local Rayleigh number, defined in equation (12b)
Ra_x^*	modified Rayleigh number, defined in equation (15)
Re^*	micro-scale Reynolds number, defined in equation (10a)
T	temperature
ΔT_w	wall-ambient temperature difference
u, v	Darcian velocity components
x, y	boundary layer coordinates
z	elevation measured from the lower stagnation point.

Greek symbols

α	equivalent thermal diffusivity of the fluid-saturated porous medium
β	coefficient of thermal expansion
η	similarity variable, defined in equation (18c)
θ	dimensionless temperature
λ_{1-4}	exponents introduced in equations (31), (39), (48) and (65)
μ	viscosity of the fluid
ν	kinematic viscosity of the fluid
ξ_{1-4}	variables defined in equations (32), (40), (49) and (66)
ρ	density of the fluid
ψ	stream function.

the Forchheimer free convection regime, the Darcian free convection regime and the forced convection regime. Appropriate dimensionless groups for distinguishing these regimes are found to be the micro-scale Reynolds and Grashof numbers based on the length scale of the micro-structure, namely, the square root of the permeability. A regime map showing these asymptotic flow regimes and their boundaries corresponding to the Darcy mixed convection, the Darcy–Forchheimer free convection and the Forchheimer mixed convection regime, has been constructed taking the micro-Reynolds number and the micro-Grashof number as the ordinate and abscissa variables.

GOVERNING EQUATIONS AND BOUNDARY CONDITIONS

In Fig. 1, we shall consider a plane or axisymmetric body of arbitrary shape, embedded in a fluid-saturated porous medium. The geometry and wall temperature of the heated body are specified by the functions of the boundary layer coordinate x, namely, $r(x)$ and $T_w(x)$. The external velocity $u_e(x)$ for the given geometry $r(x)$ may readily be obtained from the potential flow theory.

Under the boundary layer coordinates (x, y), the governing equations, namely, the equation of continuity, the non-Darcy flow model (i.e. Ergun model [14]) and the energy equation are given by

$$\frac{\partial r^* u}{\partial x} + \frac{\partial r^* v}{\partial y} = 0 \quad (1)$$

$$\frac{\mu}{K} u + \frac{\rho C}{\sqrt{K}} u^2 = -\frac{dp}{dx} - \rho g_x + \rho g_x \beta (T - T_e) \quad (2)$$

and

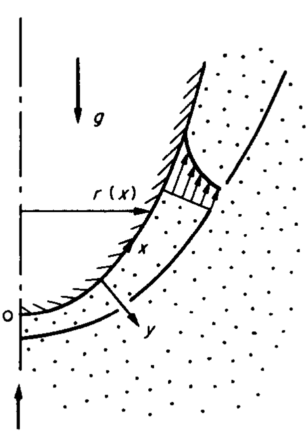

FIG. 1. Physical model and its coordinates.

$$u\frac{\partial T}{\partial x}+v\frac{\partial T}{\partial y}=\alpha\frac{\partial^2 T}{\partial y^2} \tag{3}$$

where

$$r^*=\begin{cases}1: & \text{plane flow}\\ r(x): & \text{axisymmetric flow}\end{cases} \tag{4}$$

and

$$g_x=g\left[1-\left(\frac{\mathrm{d}r}{\mathrm{d}x}\right)^2\right]^{1/2}. \tag{5}$$

In the foregoing equations, u and v are the Darcian velocity components, while T is the local temperature. The Boussinesq approximation is evoked for the buoyancy force. Furthermore, g_x is the tangential component of the acceleration due to gravity g; K the permeability; C an empirical constant associated with the non-Darcy porous inertia term; ρ the fluid density; μ the fluid viscosity; α the equivalent thermal diffusivity of the fluid saturated porous medium; β the coefficient of thermal expansion. The corresponding boundary conditions are

$$y=0:\quad v=0,\ T=T_w(x) \tag{6a,b}$$

$$y\to\infty:\quad u=u_e(x),\ T=T_e. \tag{6c,d}$$

Let us write equation (2) along the boundary layer edge ($y\to\infty$) utilizing the boundary conditions, equations (6c) and (6d)

$$-\frac{\mathrm{d}p}{\mathrm{d}x}-\rho g_x=-\frac{\mathrm{d}}{\mathrm{d}x}(p+\rho g z)=\frac{\mu}{K}u_e+\frac{\rho C}{\sqrt{K}}u_e^2 \tag{7}$$

where z is the elevation measured from the front stagnation point. The foregoing equation may be substituted into equation (2) to eliminate the pressure term as

$$\frac{\mu}{K}u+\frac{\rho C}{\sqrt{K}}u^2=\frac{\mu}{K}u_e+\frac{\rho C}{\sqrt{K}}u_e^2+\rho g_x\beta(T-T_e). \tag{8}$$

The foregoing quadratic equation may be solved for u as

$$u=\frac{v}{2C\sqrt{K}}\left[\left[(1+2Re^*)^2+4Gr^*\left(\frac{T-T_e}{\Delta T_w}\right)\right]^{1/2}-1\right] \tag{9}$$

where

$$Re^*(x)=C\sqrt{K}u_e/v \tag{10a}$$

$$Gr^*(x)=CK^{3/2}g_x\beta\Delta T_w/v^2 \tag{10b}$$

and

$$\Delta T_w(x)=T_w-T_e. \tag{10c}$$

Hence, the slip velocity at the wall u_w is given by

$$u_w=\frac{v}{2C\sqrt{K}}[[(1+2Re^*)^2+4Gr^*]^{1/2}-1] \tag{11}$$

where Re^* and Gr^* are what we may call the 'micro-scale' Reynolds and Grashof numbers, respectively, in which the reference length scale is chosen to be the length scale of the micro-structure, namely, the square root of the permeability of the porous medium.

MODIFIED PECLET NUMBER AND FLOW REGIME MAP

Most previous studies on mixed convection correlate the local Nusselt number in terms of either the local Peclet number

$$Pe_x=u_e x/\alpha \tag{12a}$$

(for the forced flow dominated case), or the local Rayleigh number

$$Ra_x=Kg_x\beta\Delta T_w x/\alpha v \tag{12b}$$

(for the buoyancy force dominated case). However, any mixed convection analysis which uses either Pe_x or Ra_x inevitably suffers from a singularity under a certain physical limiting condition. (For example, if Pe_x is used for scaling, a singularity will appear as $Ra_x/Pe_x\to\infty$.) Moreover, the velocity field is established as the result of both the external flow and the buoyancy force. Naturally, it is the total velocity magnitude over the heat transfer surface that virtually determines convective heat transfer from the heated surface. Thus, in our unified treatment, we shall choose the slip velocity at the wall as a velocity scale, and propose a new dimensionless number, namely, the modified Peclet number

$$Pe_x^*=\frac{u_w x}{\alpha}=Pe_x\frac{[(1+2Re^*)^2+4Gr^*]^{1/2}-1}{2Re^*} \tag{13}$$

to correlate the local Nusselt number. It can easily be shown that Pe_x^* transforms itself into

$$Pe_x^*=Pe_x \text{ for } Re^*+Re^{*2}\gg Gr^*$$

(I: forced convection regime) (14a)

$$Pe_x^*=Ra_x \text{ for } Re^*\ll Gr^*\ll 1$$

(II: Darcian free convection regime) (14b)

$$Pe_x^*=Ra_x^{*1/2} \text{ for } Re^*+Re^{*2}\ll Gr^* \text{ and } Gr^*\gg 1$$

(III: Forchheimer free convection regime) (14c)

where

$$Ra_x^*=\sqrt{K}g_x\beta\Delta T_w x^2/C\alpha^2 \tag{15}$$

may be identified with the new dimensionless number that Bejan and Poulikakos [7] found through a scale argument.

The foregoing three flow regimes, namely, the forced convection regime, the Darcy free convection regime and the Forchheimer free convection regime, are identified by I, II and III, respectively, in Fig. 2. Another three distinct regimes (connecting the foregoing three regimes), namely, the Darcy mixed convection regime (IV), the Darcy–Forchheimer free convection regime (V) and the Forchheimer mixed

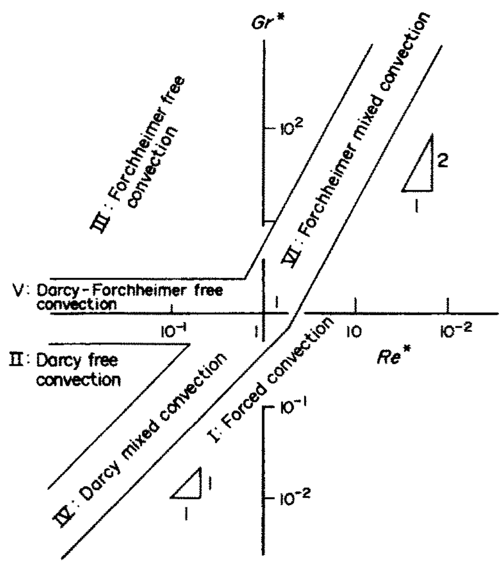

FIG. 2. Flow regime map.

convection regime (VI), may be identified, in which

$$Pe_x^* = Pe_x + Ra_x \text{ for } Gr^* \sim Re^* \ll 1$$

(IV: Darcy mixed convection regime) (16a)

$$Pe_x^* = Ra_x \frac{(1+4Gr^*)^{1/2}-1}{2Gr^*}$$

for $Gr^* \sim 1$ and $Re^* \ll 1$

(V: Darcy–Forchheimer free convection regime) (16b)

$$Pe_x^* = (Pe_x^2 + Ra_x^*)^{1/2} \text{ for } Gr^* \sim Re^{*2} \gg 1$$

(VI: Forchheimer mixed convection regime). (16c)

Thus, the modified Peclet number Pe_x^* reduces to appropriate dimensionless numbers, corresponding to the values of the micro-scale dimensionless numbers, Re^* and Gr^*. We have introduced three macro-scale dimensionless numbers and two micro-scale dimensionless numbers. However, only three among these five dimensionless numbers are independent, since we have the following inter-relations between the macro- and micro-dimensionless numbers:

$$Gr^*/Re^* = Ra_x/Pe_x \tag{17a}$$

and

$$Gr^*/Re^{*2} = Ra_x^*/Pe_x^2. \tag{17b}$$

UNIFIED TREATMENT FOR TRANSFORMING EQUATIONS

Having established the modified Peclet number Pe_x^*, we shall propose the following transformations:

$$\psi = \alpha r^*(Pe_x^* I)^{1/2} f(x,\eta) \tag{18a}$$

$$T - T_e = \Delta T_w \theta(x,\eta) \tag{18b}$$

and

$$\eta = \frac{y}{x}(Pe_x^*/I)^{1/2} \tag{18c}$$

where

$$I = \frac{\int_0^x \Delta T_w^2 u_w r^{*2}\, dx}{\Delta T_w^2 u_w r^{*2} x} \tag{19}$$

and ψ is the stream function such that

$$u = \frac{1}{r^*}\frac{\partial \psi}{\partial y} \tag{20a}$$

and

$$v = -\frac{1}{r^*}\frac{\partial \psi}{\partial x}. \tag{20b}$$

Thus, the continuity equation (1) is automatically satisfied. The proposed pseudo-similarity variable is denoted by η. The function I as defined by equation (19) adjusts the scale in the y-direction according to a given body geometry $r^*(x)$ and its surface temperature distribution.

Substitution of equations (18a)–(18c) into equations (3), (6) and (9) yields

$$f' = \frac{[(1+2Re^*)^2 + 4Gr^*\theta]^{1/2} - 1}{[(1+2Re^*)^2 + 4Gr^*]^{1/2} - 1} \tag{21}$$

and

$$\theta'' + (\tfrac{1}{2} - nI) f\theta' - nIf'\theta = Ix\left(f'\frac{\partial \theta}{\partial x} - \theta'\frac{\partial f}{\partial x}\right). \tag{22}$$

The primes in the foregoing equations denote differentiation with respect to η. The boundary conditions are

$$\eta = 0: \quad f = 0, \theta = 1 \tag{23a,b}$$

$$\eta \to \infty: \quad \theta = 0. \tag{23c}$$

The Darcian velocities are given by

$$u = u_w f' \tag{24a}$$

and

$$v = \frac{\alpha}{x}(Pe_x^*/I)^{1/2}\left[\left(nI - \frac{1}{2}\right)f + \left(\frac{1}{2} - nI - I\frac{d \ln u_w r^*}{d \ln x}\right)\eta f' - Ix\frac{\partial f}{\partial x}\right] \tag{24b}$$

where

$$n(x) = \frac{d \ln \Delta T_w}{d \ln x}. \tag{25}$$

Equation (21) may be integrated with the aid of equation (23a) as

$$f(x,\eta) = \frac{\int_0^\eta [(1+2Re^*)^2+4Gr^*\,\theta]^{1/2}\,d\eta-\eta}{[(1+2Re^*)^2+4Gr^*]^{1/2}-1}. \quad (26)$$

The resulting set of transformed equations (26) and (22) subjected to equations (23b) and (23c) includes all possible solutions to free, forced and mixed convection problems of Darcian and non-Darcian fluids. Once the temperature distribution θ is known by solving the set of transformed equations, we may evaluate the local Nusselt number of our primary concern from

$$Nu_x = \frac{q_w x}{\Delta T_w k} = -\theta'(x,0)(Pe_x^*/I)^{1/2}. \quad (27)$$

RESULTS AND DISCUSSION

In what follows, we shall consider possible physical limiting conditions, and obtain useful asymptotic expressions for Nu_x.

Forced convection regime (Regime I: $Re^*+Re^{*2} \gg Gr^*$)

The physical limiting condition, $Re^*+Re^{*2} \gg Gr^*$, reduces equations (11), (26) and (19) to

$$u_w = u_e \quad (28)$$

$$f = \eta \quad (29)$$

and

$$nI = \frac{d\ln \Delta T_w}{d\ln x}\,\frac{\int_0^x \Delta T_w^2 u_e r^{*2}\,dx}{\Delta T_w^2 u_e r^{*2} x} \equiv \frac{\lambda_1}{1+2\lambda_1}. \quad (30)$$

The preceding expression suggests that similarity solutions are possible when ΔT_w varies according to

$$\Delta T_w \propto \xi_1^{\lambda_1} \quad (31)$$

where

$$\xi_1 \equiv \int_0^x u_e r^{*2}\,dx \quad (32)$$

such that the exponent λ_1 and the product nI remain constant. Equation (27) for this particular case, reduces to

$$Nu_x = -\theta'(0)(1+2\lambda_1)^{1/2}\left(\frac{d\ln\xi_1}{d\ln x}\right)^{1/2} Pe_x^{1/2} \quad (33)$$

where $\theta'(0)$ should be found from the ordinary differential equation reduced from equation (22), namely

$$\theta''+\frac{1}{2(1+2\lambda_1)}\eta\theta'-\frac{\lambda_1}{1+2\lambda_1}\theta = 0 \quad (34)$$

subjected to equations (23b) and (23c). $d\ln\xi_1/d\ln x$ in equation (33) may readily be evaluated for any particular geometry. Especially for a vertical flat plate, we have $d\ln\xi_1/d\ln x = 1$. Thus, the present unified treatment transforms all possible similar flow cases to the vertical flat plate flow case. The non-Darcy flow expression (33) turns out to be identical to the Darcy flow expression reported in Nakayama and Koyama [5], where the local heat flux distributions over a non-isothermal wedge, cone, sphere and horizontal circular cylinder may be found. It is interesting to note that the slug flow heat transfer expression for the Darcy flows is directly applicable for the case of non-Darcy forced convection. (But see equation (7) that the pressure drop under the same u_e increases for the non-Darcy flow case.) To conclude this section, let us write equation (33) for the isothermal wall case (i.e. $\lambda_1 = 0$) as

$$Nu_x = \frac{1}{\pi^{1/2}}\left(\frac{d\ln\xi_1}{d\ln x}\right)^{1/2} Pe_x^{1/2}\ \text{(isothermal wall)}. \quad (35)$$

Darcy free convection regime (Regime II: $Re^* \ll Gr^* \ll 1$)

Since the initial study on a vertical flat plate by Cheng and Minkowycz [1], a considerable number of investigations have been carried out to seek similar and non-similar solutions (e.g. Merkin [3], and Nakayama and Koyama [2]). In this regime, the general equations (11), (26) and (19) reduce to

$$u_w = Kg_x\beta\Delta T_w/\nu \quad (36)$$

$$f = \int_0^\eta \theta\,d\eta \quad (37)$$

and

$$nI = \frac{d\ln\Delta T_w}{d\ln x}\,\frac{\int_0^x \Delta T_w^3 g_x r^{*2}\,dx}{\Delta T_w^3 g_x r^{*2} x} \equiv \frac{\lambda_2}{1+3\lambda_2}. \quad (38)$$

Similarity solutions exist when the wall temperature varies as

$$\Delta T_w \propto \xi_2^{\lambda_2} \quad (39)$$

where

$$\xi_2 \equiv \int_0^x g_x r^{*2}\,dx. \quad (40)$$

Equation (27) for this case reduces to

$$Nu_x = -\theta'(0)(1+3\lambda_2)^{1/2}\left(\frac{d\ln\xi_2}{d\ln x}\right)^{1/2} Ra_x^{1/2} \quad (41)$$

where $\theta'(0)$ should be determined from

$$\theta''+\frac{1+\lambda_2}{2(1+3\lambda_2)}\theta'\left(\int_0^\eta\theta\,d\eta\right)-\frac{\lambda_2}{1+3\lambda_2}\theta^2 = 0. \quad (42)$$

Especially for the isothermal wall, we have

$$Nu_x = 0.444\left(\frac{d\ln\xi_2}{d\ln x}\right)^{1/2} Ra_x^{1/2}\ \text{(isothermal wall)}. \quad (43)$$

The results obtained in this section are the same as those found in ref. [2], where many examples including the Darcy free convection over ellipses and ellipsoids are illustrated.

Forchheimer free convection regime (*Regime III*: $Re^* + Re^{*2} \ll Gr^*$ *and* $Gr^* \gg 1$)

Only a limited number of cases were reported for this non-Darcy flow regime [7, 15]. Let us find all possible similarity solutions from our general expressions. Equations (11), (26) and (19) for this regime become

$$u_w = (\sqrt{K} g_x \beta \Delta T_w / C)^{1/2} \tag{44}$$

$$f = \int_0^\eta \theta^{1/2} \, d\eta \tag{45}$$

and

$$nI = \frac{d \ln \Delta T_w}{d \ln x} \frac{\int_0^x \Delta T_w^{5/2} g_x^{1/2} r^{*2} \, dx}{\Delta T_w^{5/2} g_x^{1/2} r^{*2} x} \equiv \frac{\lambda_3}{1 + \frac{5}{2}\lambda_3} \tag{46}$$

where

$$\xi_3 \equiv \int_0^x g_x^{1/2} r^{*2} \, dx. \tag{47}$$

Thus, a class of similarity solutions exists when the wall temperature varies according to

$$\Delta T_w \propto \xi_3^{\lambda_3}. \tag{48}$$

The heat transfer function, equation (27), for this case, becomes

$$Nu_x = -\theta'(0)(1 + \tfrac{5}{2}\lambda_3)^{1/2} \left(\frac{d \ln \xi_3}{d \ln x} \right)^{1/2} Ra_x^{*\,1/4} \tag{49}$$

where $\theta'(0)$ should be determined from

$$\theta'' + \frac{2 + \lambda_3}{2(2 + 5\lambda_3)} \theta' \left(\int_0^\eta \theta^{1/2} \, d\eta \right) - \frac{2\lambda_3}{2 + 5\lambda_3} \theta^{3/2} = 0. \tag{50}$$

The equation under boundary conditions (23b) and (23c) can easily be solved using a standard integration procedure. For the isothermal wall (i.e. $\lambda_3 = 0$), we obtain $-\theta'(0) = 0.494$. Hence, we have

$$Nu_x = 0.494 \left(\frac{d \ln \xi_3}{d \ln x} \right)^{1/2} Ra_x^{*\,1/4} \text{ (isothermal wall).} \tag{51}$$

Unlike in the case of Darcy free convection, the heat flux at the front stagnation point of a blunt body is estimated as infinity, as equation (51) suggests that the boundary layer vanishes there.

As pointed out by Bejan and Poulikakos [7], this Forchheimer flow situation is more likely to prevail when the flow is sufficiently fast that the boundary layer approximations are relevant. We numerically integrated equation (51) to obtain the overall Nusselt number Nu on a horizontal circular cylinder and plotted the results in Fig. 3 with the experimental data by Fand *et al.* [16]. The results based on Darcy's law are also indicated for reference. It is clearly seen that the Forchheimer flow assumption gives a more reasonable level of the heat transfer rate than the Darcy flow model, even when the micro-Grashof number Gr^* is of an order of unity. (Thus, the authors feel that one of the requirements, $Gr^* \gg 1$ for the Forchheimer free convection flow, may be somewhat relaxed for practical heat transfer estimations.)

So far, we have investigated three distinct flow regimes, namely, the forced convection regime, the Darcy free convection regime and the Forchheimer free convection regime, and obtained all possible similarity solutions. In what follows, we shall consider the intermediate regimes, namely, the Darcy mixed convection regime, the Darcy–Forchheimer free convection regime and the Forchheimer mixed convection regime, bridging the aforementioned three asymptotic flow regimes. We shall see that the requirements for these intermediate flow regimes are naturally more restrictive.

Darcy mixed convection regime (*Regime IV*: $Gr^* \sim Re^* \ll 1$)

Many investigators such as Cheng [4] and Nakayama and Koyama [5] attacked the problems of the Darcy mixed convection using the local Peclet number to form a similarity variable. In their analyses, however, the asymptotic solutions for the buoyancy dominated flows were not possible, since the Peclet number vanishes under such a condition. The present unified treatment, as can be seen from equation (16a), never suffers from such singularities.

In this mixed convection regime, equations (11), (26) and (19) reduce to

$$u_w = u_e + K g_x \beta \Delta T_w / \nu \tag{52}$$

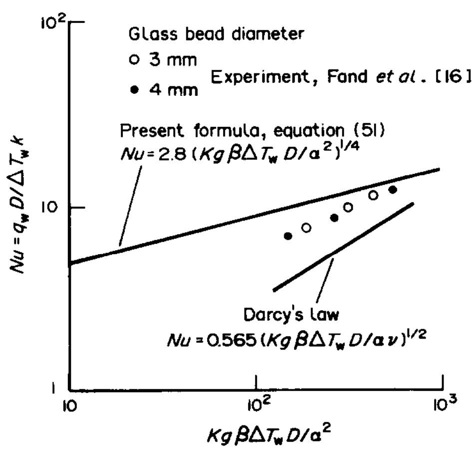

FIG. 3. Nusselt number on a horizontal circular cylinder.

$$f = \frac{Re^* \eta + Gr^* \int_0^\eta \theta \, d\eta}{Re^* + Gr^*} \tag{53}$$

and

$$nI = \frac{d \ln \Delta T_w}{d \ln x} \frac{\int_0^x \Delta T_w^2 u_e r^{*2}(1 + Gr^*/Re^*) \, dx}{\Delta T_w^2 u_e r^{*2}(1+Gr^*/Re^*)x} \equiv \frac{\lambda_1}{1+2\lambda_1}$$

$$= \frac{d \ln \Delta T_w}{d \ln x} \frac{\int_0^x \Delta T_w^3 g_x r^{*2}(1 + Re^*/Gr^*) \, dx}{\Delta T_w^3 g_x r^{*2}(1+Re^*/Gr^*)x} \equiv \frac{\lambda_2}{1+3\lambda_2}. \tag{54}$$

Thus, similarity solutions are allowed only when

$$Gr^*/Re^* (= Ra_x/Pe_x) \propto \Delta T_w g_x/u_e = \text{const.} \tag{55}$$

and

$$\Delta T_w \propto \xi_1^{\lambda_1} \tag{56a}$$

or equivalently

$$\Delta T_w \propto \xi_2^{\lambda_2}. \tag{56b}$$

Subsequently, we have

$$Nu_x = (-\theta'(0)/I^{1/2})(Pe_x + Ra_x)^{1/2} \tag{57}$$

where

$$1/I = (1+2\lambda_1)\frac{d \ln \xi_1}{d \ln x} = (1+3\lambda_2)\frac{d \ln \xi_2}{d \ln x}. \tag{58}$$

The previous study on this flow regime [5] reveals that only a limited number of similarity solutions are possible because of the very much restrictive requirements (55) and (56). Similarity solutions are found for an isothermal cylinder or sphere, and a vertical wedge or cone with its surface temperature varying with the same power index as that of the boundary layer edge velocity.

In general, $-\theta'(0)$ must be determined numerically from equation (22) with equations (53) and (54) substituted for. (Note, all right-hand side terms in equation (22) vanish for similarity solutions.) For the isothermal wall, however, the following approximate formula, which closely follows the numerical integration results, may be adequate:

$$-\theta'(0) = \frac{1}{\pi^{1/2}} \left(\frac{1 + 0.62Gr^*/Re^*}{1 + Gr^*/Re^*} \right)^{1/2}. \tag{59}$$

Hence

$$Nu_x = \frac{1}{\pi^{1/2}} \left(\frac{d \ln \xi_1}{d \ln x} \right)^{1/2} (Pe_x + 0.62Ra_x)^{1/2} \quad \text{(isothermal wall)} \tag{60}$$

where $d \ln \xi_1 / d \ln x = d \ln \xi_2 / d \ln x$ since relation (55), $g_x \propto u_e$ under the isothermal wall, must hold. The foregoing Nu_x expression asymptotically reduces to equation (35) for $Ra_x/Pe_x \to 0$ and equation (43) for $Ra_x/Pe_x \to \infty$. As observed in Fig. 4, expression (60) closely approximates the exact solution [5].

Darcy–Forchheimer free convection regime (*Regime V*: $Gr^* \sim 1$ *and* $Re^* \ll 1$)

Plumb and Huenefeld [8] were the first to find a similarity solution for an isothermal flat plate in this non-Darcy flow regime. Another class of similarity solutions was found by Nakayama *et al.* [9] for curved surfaces where the wall temperature decreases in the streamwise direction. However, the isothermal flat plate solution appears to be the only similarity solution of physical interest.

Let us generate the similarity solutions from the general equations (11), (26) and (19) as

$$u_w = \frac{\nu}{2CK^{1/2}}[(1+4Gr^*)^{1/2} - 1] \tag{61}$$

$$f = \frac{\int_0^\eta (1+4Gr^*\theta)^{1/2} \, d\eta - \eta}{(1+4Gr^*)^{1/2} - 1} \tag{62}$$

and

$$nI = \frac{d \ln \Delta T_w}{d \ln x} \frac{\int_0^x \Delta T_w^2 r^{*2}[(1+4Gr^*)^{1/2} - 1] \, dx}{\Delta T_w^2 r^{*2}[(1+4Gr^*)^{1/2} - 1]x} \equiv \frac{\lambda_4}{1+2\lambda_4}. \tag{63}$$

For the product nI to be constant, we must satisfy

$$Gr^* \propto g_x \Delta T_w = \text{const.} \tag{64}$$

and

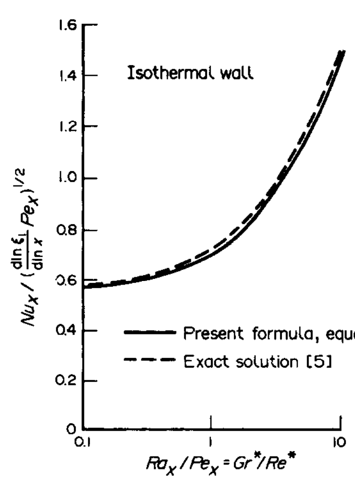

FIG. 4. Heat transfer results on Darcy mixed convection.

$$\Delta T_w \propto \xi_4^{\lambda_4} \tag{65}$$

where

$$\xi_4 \equiv \int_0^x r^{*2}\,\mathrm{d}x. \tag{66}$$

Thus, we have obtained the same similarity requirements as already found in the previous study [9]. The local Nusselt number for this non-Darcy free convection regime is given by

$$Nu_x = -\theta'(0)(1+2\lambda_4)^{1/2}\left(\frac{\mathrm{d}\ln\xi_4}{\mathrm{d}\ln x}\right)^{1/2} \times\left(Ra_x\frac{(1+4Gr^*)^{1/2}-1}{2Gr^*}\right)^{1/2}. \tag{67}$$

Especially for the isothermal case, we propose the following approximate formula:

$$Nu_x = \frac{[16Gr^{*2}-[(1+4Gr^*)^{1/2}-1]^2]^{1/2}}{8Gr^*}\left(\frac{\mathrm{d}\ln\xi_4}{\mathrm{d}\ln x}\right)^{1/2} \times\left(Ra_x\frac{(1+4Gr^*)^{1/2}-1}{2Gr^*}\right)^{1/2}\ \text{(isothermal wall)} \tag{68}$$

where $-\theta'(0)$ has been approximated by modifying the Bejan–Poulikakos formula [7] based on Oseen's linearized solution, such that it closely follows the asymptotic expressions, namely, equation (43) for $Gr^* \ll 1$ and equation (51) for $Gr^* \gg 1$. (Note $\mathrm{d}\ln\xi_4/\mathrm{d}\ln x = \mathrm{d}\ln\xi_2/\mathrm{d}\ln x = \mathrm{d}\ln\xi_3/\mathrm{d}\ln x$, since the relation $g_x \propto 1/\Delta T_w = \text{const.}$ must hold for this isothermal case.) The proposed formula for the isothermal wall is shown along with the exact values [7] in Fig. 5, where excellent agreement between the formula and exact values can be seen.

Forchheimer mixed convection regime (Regime VI: $Gr^* \sim Re^{*2} \gg 1$)

Only a limited number of non-Darcy mixed convection problems have been treated so far. Recently, Kumari and Nath [13] attacked the mixed convection over an isothermal vertical cylinder in a porous medium, retaining both the Darcy and Forchheimer terms. The heat transfer results were obtained for the

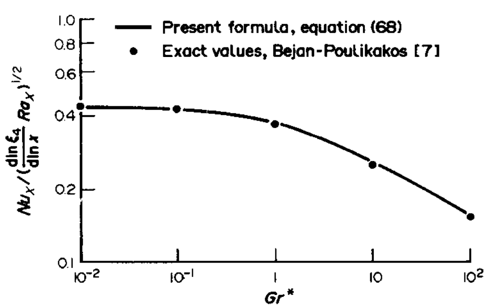

FIG. 5. Heat transfer results on Darcy–Forchheimer free convection.

specific case of $Re^* = 1$, with Gr^* varying from 0.1 to 100. Let us investigate this unexplored flow regime.

The general expressions (11), (26) and (19), in this flow regime, reduce to

$$u_w = (u_e^2 + K^{1/2}g_x\beta\Delta T_w/C)^{1/2} \tag{69}$$

$$f = \frac{\int_0^\eta (Re^{*2}+Gr^*\,\theta)^{1/2}\,\mathrm{d}\eta}{(Re^{*2}+Gr^*)^{1/2}} \tag{70}$$

and

$$nI = \frac{\mathrm{d}\ln\Delta T_w}{\mathrm{d}\ln x}\frac{\int_0^x \Delta T_w^2 u_e r^{*2}(1+Gr^*/Re^{*2})\,\mathrm{d}x}{\Delta T_w^2 u_e r^{*2}(1+Gr^*/Re^{*2})x} \equiv \frac{\lambda_1}{1+2\lambda_1}$$

$$= \frac{\mathrm{d}\ln\Delta T_w}{\mathrm{d}\ln x}\frac{\int_0^x \Delta T_w^{5/2}g_x^{1/2}r^{*2}(1+Re^{*2}/Gr)\,\mathrm{d}x}{\Delta T_w^{5/2}g_x^{1/2}r^{*2}(1+Re^{*2}/Gr^*)x} \equiv \frac{\lambda_3}{1+\frac{5}{2}\lambda_3}. \tag{71}$$

Thus, similarity solutions are possible only when

$$Gr^*/Re^{*2}(=Ra_x^*/Pe_x^2) \propto \Delta T_w g_x/u_e^2 = \text{const.} \tag{72}$$

and

$$\Delta T_w \propto \xi_1^{\lambda_1} \tag{73a}$$

or equivalently

$$\Delta T_w \propto \xi_3^{\lambda_3}. \tag{73b}$$

Correspondingly, we have

$$Nu_x = (-\theta'(0)/I^{1/2})(Pe_x^2 + Ra_x^*)^{1/4} \tag{74}$$

where

$$1/I = (1+2\lambda_1)\frac{\mathrm{d}\ln\xi_1}{\mathrm{d}\ln x} = (1+\tfrac{5}{2}\lambda_3)\frac{\mathrm{d}\ln\xi_3}{\mathrm{d}\ln x}. \tag{75}$$

Let us consider possible situations where requirements (72) and (73) are satisfied. The potential flow theory tells that the free stream velocity over a wedge or a cone varies according to $u_e \propto x^m$, where the exponent m is some function of the wedge angle or the cone apex angle. Since g_x is constant for a vertical wedge or a cone, pointing downward, we must have $\Delta T_w \propto x^{2m}$ (i.e. $n = 2m$) for requirement (72) to be satisfied. The other requirement (73) may be used to find the value of either λ_1 or λ_3. Thus, for these similar flow cases, the product nI needed for the solution of equation (22) becomes a function of m as

$$nI = \frac{2m}{1+5m}\ \text{for a vertical wedge} \tag{76a}$$

and

$$nI = \frac{2m}{3+5m}\ \text{for a vertical cone.} \tag{76b}$$

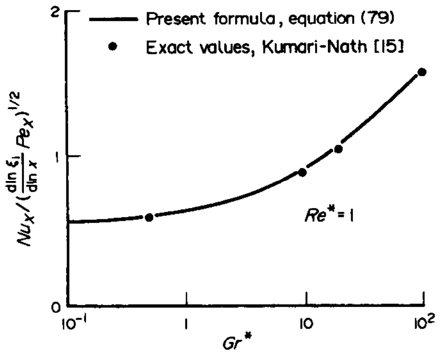

FIG. 6. Heat transfer results on Forchheimer mixed convection.

In a similar fashion, we can show that the flow around the front stagnation point of a horizontal circular cylinder or a sphere with its wall temperature varying according to $\Delta T_w \propto \sin(x/R)$ (where R is the radius) admits similarity solutions. The product nl for these stagnation regions should be set to

$$nl = 1/4 \text{ for a horizontal circular cylinder} \quad (77a)$$

and

$$nl = 1/6 \text{ for a sphere.} \quad (77b)$$

Equation (22) with equation (70) and nl given by (76) or (77) can easily be solved numerically to find $-\theta'(0)$. However, for the isothermal case (i.e. $nl = 0$), we propose the following approximate formula which can conveniently be used for heat transfer estimation with a sufficient accuracy:

$$-\theta'(0) = \frac{1}{\pi^{1/2}}\left(\frac{1+0.59Gr^*/Re^{*2}}{1+Gr^*/Re^{*2}}\right)^{1/4}. \quad (78)$$

Hence

$$Nu_x = \frac{1}{\pi^{1/2}}\left(\frac{\mathrm{d}\ln\xi_1}{\mathrm{d}\ln x}\right)^{1/2}(Pe_x^2+0.59Ra_x^*)^{1/4}$$

$$\text{(isothermal wall)} \quad (79)$$

where $\mathrm{d}\ln\xi_1/\mathrm{d}\ln x = \mathrm{d}\ln\xi_3/\mathrm{d}\ln x$ since relation (72), namely, $u_e \propto g_x^{1/2}$ under the isothermal wall, must hold. The above formula naturally generates the asymptotic expression for the forced convection regime (i.e. equation (35)) as $Ra_x^*/Pe_x^2 \to 0$, and that for the Forchheimer free convection regime (i.e. equation (51)) as $Ra_x^*/Pe_x^2 \to \infty$.

The vertical cylinder results obtained for a fixed Re^* value (i.e. $Re^* = 1$) by Kumari and Nath [13] belong to the ordinate axis of the flow regime map shown in Fig. 2. (Their analysis on a vertical cylinder includes the radial curvature effects. However, for large Pe_x such effects may well be neglected, and the solution reduces to the one for the vertical flat plate.) As we increase Gr^* along the ordinate axis, we go from the forced convection regime (Regime I) to the Forchheimer free convection regime (Regime III). The curve $Nu_x/Pe_x^{1/2}$ for $Re^* = 1$ was generated using the foregoing approximate equation (79), and plotted in Fig. 6 with the finite calculation results of Kumari and Nath. The figure suggests that our expression (79) is quite accurate even for the case of $Gr^* \sim 1$ originally excluded from this flow regime.

CONCLUDING REMARKS

In this article, we showed that the slip velocity at the wall resulting from the externally forced flow and the buoyancy force, virtually governs the heat transfer rate at the wall. Upon introducing a modified Peclet number based on the slip velocity, we transformed the governing equations, once for all possible cases of free, forced and mixed convection in Darcy and non-

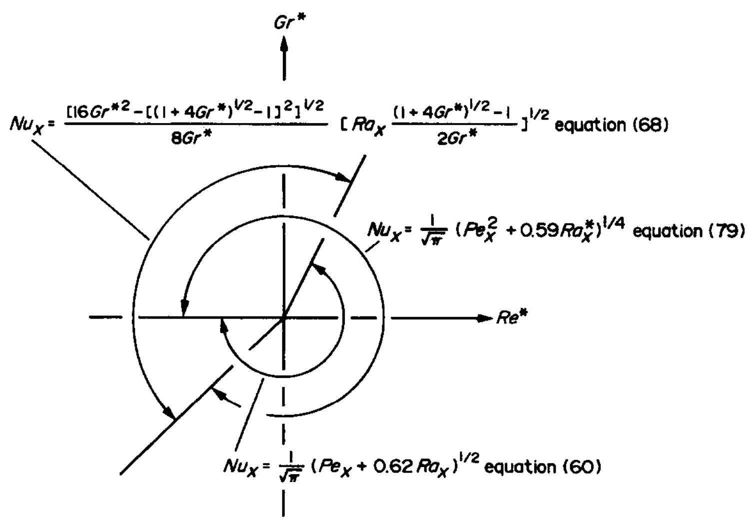

FIG. 7. Proposed heat transfer formulas for an isothermal flat plate.

Darcy porous media. This unified treatment for transformations reveals that convective flows can be classified into three flow regimes, namely, the forced convection regime, the Darcy free convection regime and the Forchheimer free convection regime, depending on the magnitudes of the micro-scale Reynolds and Grashof numbers based on the square root of the permeability. Upon considering physical limiting conditions, all possible similarity solutions for these three regimes have been extracted from the transformed governing equations, and a flow regime map based on the micro-Reynolds and Grashof number has been constructed.

Furthermore, another three intermediate flow regimes (bridging the aforementioned three regimes), namely, the Darcy mixed convection regime, the Darcy–Forchheimer free convection regime and the Forchheimer mixed convection regime have been investigated to establish the Nusselt number expressions which naturally reduce to the corresponding asymptotic expressions under appropriate physical limiting conditions. Especially, for the case of isothermal vertical flat plates (i.e. $\lambda_i = 0$ and $\mathrm{d}\ln \xi_i/\mathrm{d}\ln x = 1$ for $i = 1, 2, 3$ and 4), the three Nusselt number expressions derived for these intermediate regimes overlap onto one another, as illustrated in Fig. 7. These three expressions which guarantee sufficient accuracy may be quite useful for practical estimations of heat transfer rates. Perhaps, one should consult with the flow regime map and corresponding asymptotic expressions provided in this study, before sitting in front of a computer terminal to carry out numerical integrations for a number of sets of the flow parameters, since the flow regime map and asymptotic expressions may save a significant amount of computer time which would otherwise be necessary to perform such a parametric study.

REFERENCES

1. P. Cheng and W. J. Minkowycz, Free convection about a vertical flat plate embedded in a saturated porous medium with application to heat transfer from a dike, *J. Geophys. Res.* **82,** 2040–2044.
2. A. Nakayama and H. Koyama, Free convective heat transfer over a non-isothermal body of arbitrary shape embedded in a fluid-saturated porous medium, *J. Heat Transfer* **109,** 125–130 (1987).
3. J. H. Merkin, Free convection boundary layers on axisymmetric and two dimensional bodies of arbitrary shape in a saturated porous medium, *Int. J. Heat Mass Transfer* **22,** 1461–1462 (1979).
4. P. Cheng, Mixed convection about a horizontal cylinder and a sphere in a fluid-saturated porous medium, *Int. J. Heat Mass Transfer* **25,** 1245–1247 (1982).
5. A. Nakayama and H. Koyama, A general similarity transformation for combined free and forced convection flows within a fluid-saturated porous medium, *J. Heat Transfer* **109,** 1041–1045 (1987).
6. P. Forchheimer, Wasserbewegung durch Boden, *ForschHft. Ver Dt. Ing.* **45,** 1782–1788 (1901).
7. A. Bejan and D. Poulikakos, The non-Darcy regime for vertical boundary layer natural convection in a porous medium, *Int. J. Heat Mass Transfer* **27,** 717–722 (1984).
8. O. A. Plumb and J. C. Huenefeld, Non-Darcy natural convection from heated surfaces in saturated porous media, *Int. J. Heat Mass Transfer* **24,** 765–768 (1981).
9. A. Nakayama, H. Koyama and F. Kuwahara, Similarity solution for non-Darcy free convection from a non-isothermal curved surface in a fluid-saturated porous medium, *J. Heat Transfer* **111,** 807–811 (1989).
10. M. Kumari, I. Pop and G. Nath, Non-Darcy natural convection from a heated vertical plate in saturated porous media with mass transfer, *Int. Commun. Heat Mass Transfer* **12,** 337–346 (1985).
11. R. Vasantha, I. Pop and G. Nath, Non-Darcy natural convection over a slender vertical frustum of a cone in a saturated porous medium, *Int. J. Heat Mass Transfer* **29,** 153–156 (1986).
12. F. C. Lai and F. A. Kulacki, Non-Darcy convection from horizontal impermeable surfaces in saturated porous media, *Int. J. Heat Mass Transfer* **30,** 2189–2192 (1987).
13. M. Kumari and G. Nath, Non-Darcy mixed convection boundary layer flow on a vertical cylinder in a saturated porous medium, *Int. J. Heat Mass Transfer* **32,** 183–187 (1989).
14. S. Ergun, Fluid flow through packed columns, *Chem. Engng Prog.* **48,** 89–94 (1952).
15. D. B. Ingham, The non-Darcy free convection boundary layer on axisymmetric and two-dimensional bodies of arbitrary shape, *Int. J. Heat Mass Transfer* **29,** 1759–1763 (1986).
16. R. M. Fand, T. E. Steinberger and P. Cheng, Natural convection heat transfer from a horizontal cylinder embedded in a porous medium, *Int. J. Heat Mass Transfer* **29,** 119–133 (1986).

UNE TRANSFORMATION AFFINE UNIFIEE POUR LA CONVECTION NATURELLE OU FORCEE OU MIXTE DANS DES MILIEUX POREUX DARCYENS OU NON

Résumé—On propose une transformation affine unifiée pour extraire toutes les solutions affines possibles de la convection naturelle, ou forcée ou mixte dans des milieux poreux darcyens ou non. La vitesse de glissement à la paroi résultant de l'écoulement forcé externe et de la force de flottement est choisie comme échelle de vitesse pour former un nombre de Peclet modifié qui le transforme naturellement en nombre de Peclet conventionnel et en nombre de Rayleigh dans certaines conditions physiques particulières. Ce traitement unifié révèle trois régimes d'écoulement limitants: le régime de convection forcée, celui de convection naturelle selon Darcy et celui de convection naturelle selon Forchheimer, ainsi que trois autres régimes intermédiaires qui sont celui de convection mixte selon Darcy, celui de Darcy–Forchheimer en convection naturelle et celui de convection mixte selon Forchheimer. Pour distinguer ces régimes on a trouvé des paramètres significatifs qui sont les nombres de "micro-échelle" de Reynolds et de Grashof, basés sur la racine carrée de la perméabilité. Une carte de régime d'écoulement est construite pour montrer ces six régimes différents en portant en abscisse et en ordonnées les deux nombres adimensionnels de micro-échelle. Des expressions asymptotiques données sont très utiles pour l'estimation pratique du transfert thermique convectif dans les milieux poreux.

EINE VEREINHEITLICHTE ÄHNLICHKEITSTRANSFORMATION FÜR FREIE, ERZWUNGENE UND MISCH-KONVEKTION IN PORÖSEN MEDIEN INNERHALB UND AUSSERHALB DES DARCY'SCHEN BEREICHES

Zusammenfassung—Es wird eine vereinheitlichte Ähnlichkeitstransformation vorgeschlagen, um alle möglichen Ähnlichkeitslösungen für freie, erzwungene und Misch-Konvektion in porösen Medien innerhalb und außerhalb des Darcy'schen Bereiches zu ermitteln. Die Gleitgeschwindigkeit an der Wand aufgrund der äußeren erzwungenen Strömung und aufgrund von Auftriebskräften wird als Geschwindigkeitsmaßstab herangezogen. Damit wird eine modifizierte Peclet-Zahl gebildet, die unter bestimmten physikalischen Grenzbedingungen naturgemäß in die konventionelle Peclet- und Rayleigh-Zahl übergeht. Dieses vereinheitlichte Verfahren läßt als Extremfälle drei Strömungsbereiche erkennen: den Bereich erzwungener Konvektion, den Bereich der freien Konvektion nach Darcy und den Bereich der freien Konvektion nach Forchheimer. Dazwischen liegen drei weitere Bereiche: die Misch-Konvektion nach Darcy, die freie Konvektion (Darcy–Forchheimer) und die Misch-Konvektion nach Forchheimer. Die zur Unterscheidung dieser Strömungsgebiete relevanten Strömungsparameter sind die Reynolds- und die Grashof-Zahl für die Vorgänge im kleinen (beide beruhen auf der Quadratwurzel aus der Permeabilität). Diese beiden Kennzahlen werden auf der Abszisse bzw. auf der Ordinate aufgetragen, wodurch sich eine Strömungsbereichskarte ergibt, die die genannten sechs Strömungsgebiete zeigt. Die asymptotischen Ausdrücke, welche für diese Strömungsgebiete entwickelt worden sind, erscheinen für praktische Berechnungen des konvektiven Wärmetransports in porösen Medien innerhalb und außerhalb des Darcy'schen Bereiches nützlich.

ОБОБЩЕННОЕ ПРЕОБРАЗОВАНИЕ ПОДОБИЯ ДЛЯ СВОБОДНОЙ, ВЫНУЖДЕННОЙ И СМЕШАННОЙ КОНВЕКЦИИ В КЛАССИЧЕСКИХ И НЕКЛАССИЧЕСКИХ ПОРИСТЫХ СРЕДАХ

Аннотация—Предложено обобщенное преобразование подобия, позволяющее получить все возможные решения для свободной, вынужденной и смешанной конвекции в различных пористых средах. Скорость скольжения у стенки, обусловленная вынужденным течением за счет внешних сил и подъемными силами, выбрана в качестве характерной скорости для образования модифицированного числа Пекле, которое при некоторых физических предельных условиях естественным образом переходит в обыкновенные числа Пекле и Рэлея. Описываемая обобщенная методика позволяет различить три предельных режима течения, а именно, режим вынужденной конвекции, свободноконвективное течение Дарси, свободноконвективное течение Форшхаймера, а также три промежуточных режима, а именно, смешанная конвекция Дарси, свободная конвекция Дарси–Форшхаймера и режим смешанной конвекции Форшхаймера. Найдено, что определяющими параметрами течения, различающими данные режимы, являются "микромасштабные" числа Рейнольдса и Грасгофа на основе квадратного корня величины проницаемости. Для иллюстрации шести указанных режимов течения составлена карта с использованием микромасштабных безразмерных чисел в качестве переменных абсциссы и ординаты. Полученные для данных режимов течения асимптотические выражения могут применяться для практической оценки конвективного теплопереноса в средах, подчиняющихся и не подчияющихся закону Дарси.